

This is a repository copy of *Conformational landscapes of bimesogenic compounds and their implications for the formation of modulated nematic phases*.

White Rose Research Online URL for this paper:

<https://eprints.whiterose.ac.uk/id/eprint/119965/>

Version: Published Version

Article:

Archbold, Craig Thomas, Mandle, Richard orcid.org/0000-0001-9816-9661, Andrews, Jessica L. et al. (2 more authors) (2017) Conformational landscapes of bimesogenic compounds and their implications for the formation of modulated nematic phases. LIQUID CRYSTALS. pp. 1-11. ISSN: 1366-5855

<https://doi.org/10.1080/02678292.2017.1360954>

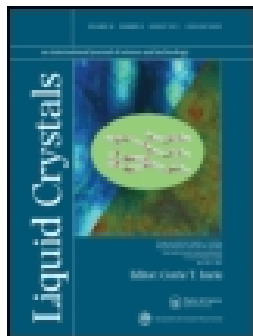
Reuse

This article is distributed under the terms of the Creative Commons Attribution (CC BY) licence. This licence allows you to distribute, remix, tweak, and build upon the work, even commercially, as long as you credit the authors for the original work. More information and the full terms of the licence here:

<https://creativecommons.org/licenses/>

Takedown

If you consider content in White Rose Research Online to be in breach of UK law, please notify us by emailing eprints@whiterose.ac.uk including the URL of the record and the reason for the withdrawal request.



Conformational landscapes of bimesogenic compounds and their implications for the formation of modulated nematic phases

Craig T. Archbold, Richard J. Mandle, Jessica L. Andrews, Stephen J. Cowling & John W. Goodby

To cite this article: Craig T. Archbold, Richard J. Mandle, Jessica L. Andrews, Stephen J. Cowling & John W. Goodby (2017): Conformational landscapes of bimesogenic compounds and their implications for the formation of modulated nematic phases, Liquid Crystals, DOI: [10.1080/02678292.2017.1360954](https://doi.org/10.1080/02678292.2017.1360954)

To link to this article: <http://dx.doi.org/10.1080/02678292.2017.1360954>



© 2017 The Author(s). Published by Informa UK Limited, trading as Taylor & Francis Group.



[View supplementary material](#)



Published online: 02 Aug 2017.



[Submit your article to this journal](#)



Article views: 62




[View related articles](#)



[View Crossmark data](#)

Conformational landscapes of bimesogenic compounds and their implications for the formation of modulated nematic phases

Craig T. Archbold, Richard J. Mandle , Jessica L. Andrews, Stephen J. Cowling and John W. Goodby

Department of Chemistry, University of York, York, UK

ABSTRACT

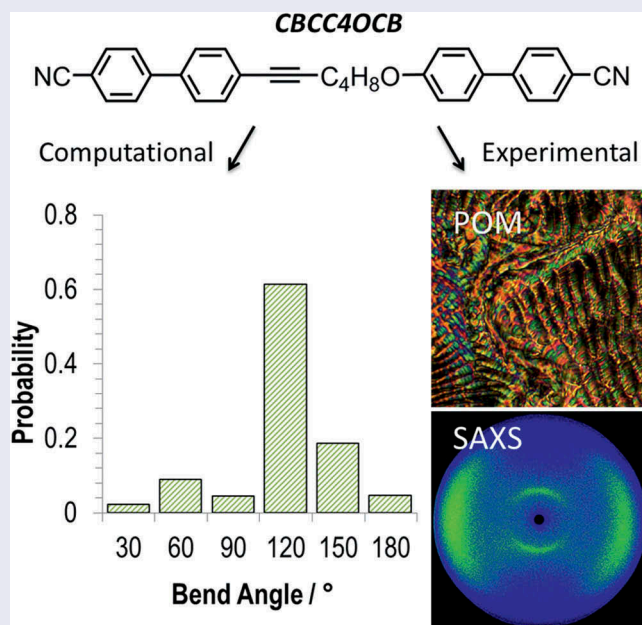
The twist-bend phase (N_{TB}) is most commonly observed in materials with a gross-bent shape: dimers; bent-cores; bent-oligomers. We had suggested previously that the bend-angle of such systems effectively dictates the relative thermal stability of the N_{TB} phase. However, our earlier paper relied on the use of a single energy-minimum conformer and so failed to capture any information about flexibility and conformational distribution. In the present work, we revisit our hypothesis and examine a second set of dimers with varying linking groups and spacer composition. We have improved on our earlier work by studying the conformational landscape of each material, allowing average bend-angles to be determined as well as the conformer distribution. We observe that the stability of the N_{TB} phase exhibits a strong dependence not only on the Boltzmann-weighted average bend-angle (rather than just a static conformer), but also on the distribution of conformers. To a lesser extent, the flexibility of the spacer appears important. Ultimately, this work satisfies both theoretical treatments and our initial experimental study and demonstrates the importance of molecular bend to the N_{TB} phase.

ARTICLE HISTORY

Received 8 June 2017

KEYWORDS

Liquid Crystal Dimers; N_{TB} ; conformations; structure-property relations




Introduction

The discovery of the twist-bend phase (N_{TB}) has given fresh impetus to the study of dimeric liquid crystals [1–13]. First predicted by Dozov [13], this liquid-crystalline state of matter has a locally helical structure with a pitch measured to be on the order of 10 nm [4,14], with this phase

displaying a number of unusual and unique optical textures [15]. When the twist-bend phase is chiral, other ‘nematic-like’ mesophases have been reported whose structure is as yet unknown [5,16], whereas a nematic-to-nematic transition has also been recently reported for a polar rod-like compound [17]. A number of reviews concerning the twist-bend phase have been published recently [18–20]. A

CONTACT Richard J. Mandle  Richard.mandle@york.ac.uk

 Supplemental data for this article can be accessed [here](#).

© 2017 The Author(s). Published by Informa UK Limited, trading as Taylor & Francis Group.

This is an Open Access article distributed under the terms of the Creative Commons Attribution License (<http://creativecommons.org/licenses/by/4.0/>), which permits unrestricted use, distribution, and reproduction in any medium, provided the original work is properly cited.

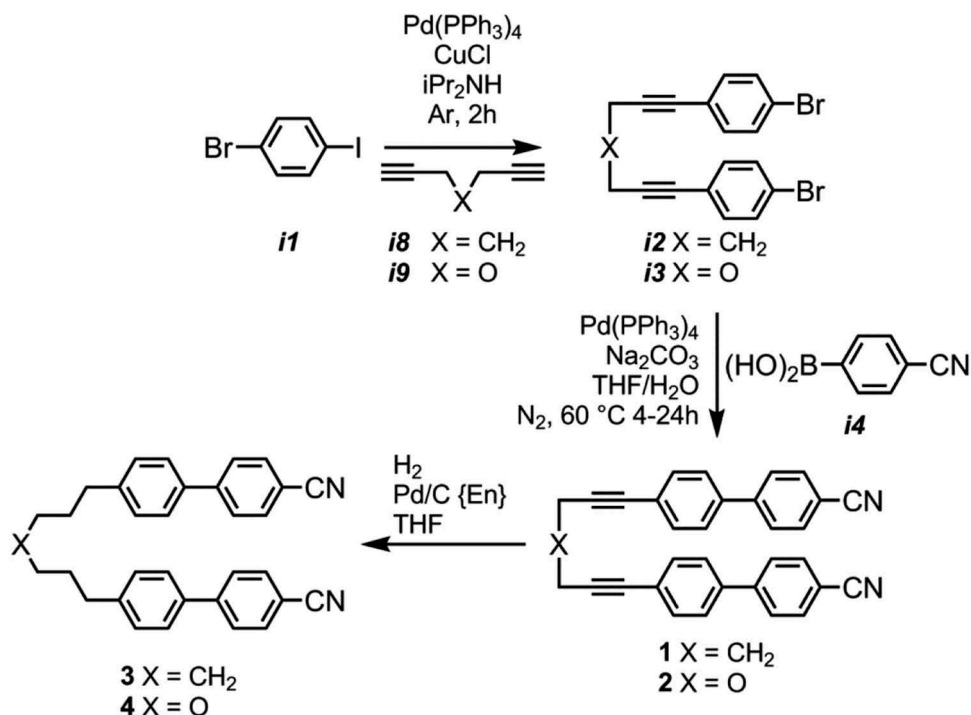
relatively large number of dimeric liquid crystals are known to exhibit this state of matter [1,3,8,9,11,12,21–30], and there is a growing number of liquid-crystalline oligomers known to exhibit the twist-bend phase [18,31–34]. Additionally, this phase has been observed in a phenylpiperazine derived bent-core liquid crystal [4].

In dimeric materials, the twist-bend phase has been demonstrated to be somewhat insensitive to the chemical composition of the mesogenic units [35] provided the overall shape is ‘bent’ [36]. In our previous demonstration of the relationship between the dimer bend-angle and the thermal stability of the twist-bend phase, we relied on a single conformer. This fails to capture any information concerning the conformational landscape and therefore makes rather large assumptions, despite being shown to be the dominant conformer by 1D ^1H NOESY NMR [36]. In this present work, we present a new set of liquid-crystalline dimesogens with varying linking-group and spacer compositions; in addition to studying the thermal behaviour by microscopy, calorimetry and X-ray scattering, we studied the conformational landscape of each material computationally, allowing us to obtain the bend-angle as a weighted average of many conformers.

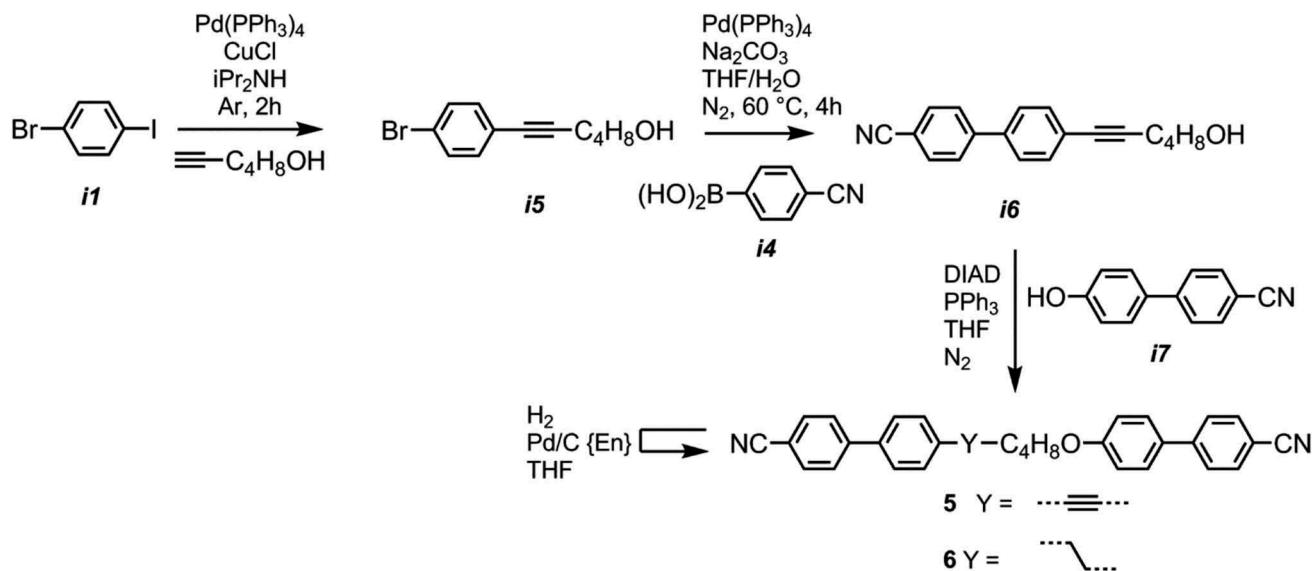
Experimental

Chemical intermediates were obtained from commercial suppliers and used without further purification.

Solvents were purchased from Fisher Scientific dried by sequential percolation through columns of activated alumina and copper Q5 catalyst prior to use. Chemical intermediates were analysed by ^1H and ^{13}C $\{^1\text{H}\}$ NMR spectroscopy, mass-spectrometry, with the purity final (i.e. liquid-crystalline) materials assayed using reverse-phase High Performance Liquid Chromatography (HPLC) or combustion analysis. Quantum chemical calculations were performed using the Gaussian 09 revision e.01 suite of programmes [37] while semi-empirical calculations were performed in either Gaussian G09 revision e.01 (AM1) or in MOPAC 2012 (PM7). Qutemol was used to visualise output files of selected conformers [38]. The small-angle X-ray scattering (SAXS) setup used is described elsewhere [39]. Compound 7 (CBO5OCB) was prepared as described by Emsley et al. [40]. Compound 10 was prepared as described by Creed et al. [41]. The diketone linked 8 was prepared as described by us previously [36]. The *bis* imine 9 was prepared by condensation of propane-1,3-diamine with 4-(4-cyanophenyl)benzaldehyde in an analogous manner to that reported by us previously [36]. Full experimental details, including characterisation of novel materials, are given in the SI to this article. A Sonogashira coupling of 4-iodobromobenzene with heptadiyne or dipropargyl ether was followed by a Suzuki–Miyaura coupling with 4-cyanophenyl boronic acid, affording 1 and 2,



Scheme 1.



Scheme 2.

respectively. A selective hydrogenation of **1** and **2** using 5% palladium on carbon poisoned with diaminoethane (Pd/C{En}) afforded **3** and **4**. The synthesis of these materials is shown in Scheme 1.

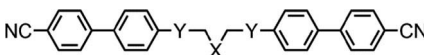
We used a similar Sonogashira/Suzuki protocol to prepare compounds **5** and **6** (CB6OCB); a Sonogashira coupling of 4-iodobromobenzene with hexyn-1-ol afforded **i5**, Suzuki coupling with 4-cyanophenylboronic acid affords the useful alcohol terminated biphenyl **i6**. Etherification with 4-hydroxy-4'-cyanobiphenyl (**i7**) via the Mitsunobu protocol afforded compound **5**, with selective hydrogenation using Pd/C{En} affording **6** (CB6OCB). The transition temperatures of the obtained material only marginally different to those reported previously [24].

Results and discussion

Compounds **1–10** were studied by a combination of polarised optical microscopy, differential scanning calorimetry (DSC) and – for selected materials – SAXS. For compound **7** (CBO5OCB), we also prepared a phase diagram for extrapolation of a virtual $N_{\text{TB}}\text{--}N$ transition temperature. The transition temperatures and associated enthalpies of transition for **1–10** are given in Table 1.

Compound **1** can be considered to be the alkyne-linked homologue of **3** (CB7CB); whereas CB7CB exhibits nematic and N_{TB} phases, **1** is non-mesogenic. Compound **2** (with the central methylene group of **1** replaced with an oxygen atom) is also non-mesogenic and appears to decompose prior to melting. The transition temperatures of **3** (CB7CB) and **6** (CB6OCB) are

in keeping with those reported previously [24]. Compound **4** can be thought of in two ways; as an isomer of **6**, where the single ether link present in the parent material has been repositioned to the centre of the spacer unit, and as being homologous in structure to CB7CB except having the centremost methylene unit replaced with an ether group. This leads to dramatic reductions in clearing point and the $N_{\text{TB}}\text{--}N$ transition temperature when compared either parent material, the reasons for which will be discussed shortly. Similarly, replacement of the methylene linking unit of **6** with an alkyne to afford **5** yields an increase in melting point and reductions in the clearing point ($\sim 8^\circ\text{C}$) and $N\text{--}N_{\text{TB}}$ transition temperature ($\sim 22^\circ\text{C}$). It has recently been reported that **7** (CBO5OCB) exhibits the twist-bend phase upon deep supercooling to $\sim 78^\circ\text{C}$ [42]. We were able to observe what we believe to be the N_{TB} phase by ejecting the sample into liquid nitrogen (i.e. rapid cooling); however, this method prevents determination of the actual transition temperature and we were unable to replicate this success when performing controlled cooling. We therefore constructed a phase diagram for binary mixtures of compound **7**/CB9CB; a plot of $T_{N_{\text{TB}}\text{--}N}$ versus concentration was constructed; whereas there is typically a linear relationship between concentration and transition temperature, we observed stabilisation of the N_{TB} phase in mixtures, as was observed much earlier by Ramou et al. [43]. An acceptable fit to the data was obtained using a quadratic function ($R^2 > 0.95$), and from this, we obtained a transition temperature value of 82°C (phase diagram and equation in ESI), in good agreement with Paterson et al. [42]. As reported by us previously the diketone-

Table 1. Transition temperatures (°C) for compounds **1–10**, and for novel compounds (**1, 2, 4, 5, 9**) associated enthalpies of transition (kJ mol^{−1}) as determined by DSC at a heat/cool rate of 10°C min^{−1}.


No.	X	Y	Y'	Cr	$T_{N_{TB}}$	N_{TB}	N	Iso
1 CBCC3CCCB	−CH ₂ −	−CC−	−CC−	•	160.5 [43.8]	−	−	•
2 CBCC101CCB	−O−	−CC−	−CC−	•	>225*	−	−	•
3 CB7CB	−CH ₂ −	−CH ₂ CH ₂ −	−CH ₂ CH ₂ −	•	104.4 [23.1]	•	106.5 [0.4]	•
4 CB3O3OCB	−O−	−CH ₂ CH ₂ −	−CH ₂ CH ₂ −	•	100.5 [13.7]	(•)	46.0 [0.01]	•
5 CBCC4OCB	−CH ₂ −	−OCH ₂ −	−CC−	•	132.8 [25.5]	(•)	97.0 [0.02]	•
6 CB6OCB	−CH ₂ −	−OCH ₂ −	−CH ₂ CH ₂ −	•	102.1 [24.2]	•	110.5 [<0.1]	•
7 CBO5OCB	−CH ₂ −	−OCH ₂ −	−CH ₂ O−	•	137.9 [25.5]	(#)	81.3 [2.1]	•
8 CBC(O)5C(O)CB	−CH ₂ −	−C(=O)−CH ₂ −	−CH ₂ −C(=O)−	•	158.1 [32.4]	(•)	145.1 [<0.1]	•
9 CB-CN3NC-CB	−CH ₂ −	−CH=N−	−N=CH−	•	170.8 [24.7]	(•)	114.9 [<0.1]	•
10 CBO2O2OCB	−O−	−OCH ₂ −	−CH ₂ O−	•	150.5 [46.2]	−	−	•

*Extensive decomposition and charring occurs at this temperature, cooling the melted (possibly decomposed) material results in crystallisation rather than a transition into a mesophase. #The material does not exhibit the N_{TB} phase in its neat state, a virtual transition temperature was obtained by constructing a phase diagram with CB9CB and then extrapolating $T_{N-N_{TB}}$ by fitting (phase diagrams in SI). Transitions in parenthesis () are monotropic, i.e. they occur below the melting point of the sample. Trivial names have been included for compounds **3, 6** and **7**.

linked cyanobiphenyl dimer, compound **8**, in this work, exhibits a significantly higher $T_{N_{TB-N}}$ and T_{N-I} than the parent compound **3**. The *bis*-imine-linked material **9** exhibits a direct isotropic to N_{TB} phase transition, and it should be noted that similar behaviour has been reported for other *bis* imine dimers with short central spacers [44,45]. As with **7**, compound **10** does not exhibit the N_{TB} phase and we observed that our transition temperatures were marginally higher than those reported previously by Creed et al. (Cr 146.5, N 153.5 Iso) [41]. A sample of **10** was ejected into liquid nitrogen, giving rapid cooling from ~175°C to cryogenic temperatures. The sample was studied via microscopy while allowed to warm to ambient temperature; however unlike **7** (CBO5OCB), we did not observe the N_{TB} phase during this forced supercooling, and we elected not to construct a phase diagram. Identification of the lower temperature phase as the twist-bend was made based on optical textures; representative photomicrographs from the compounds in Table 1 are given in Figure 1, along with a SAXS pattern for the nematic and twist-bend phase exhibited by **5**, the diffuse scattering at small angles demonstrates the nematic nature of both phases. The *d*-spacing value of the small-angle peak occurs at $Q \approx 0.5 \text{ \AA}^{-1}$ (*d*-spacing of 12.6 Å) which corresponds to approximately one half of the molecular length (26 Å from geometry optimised at the B3LYP/6-31G(d) level of DFT).

As demonstrated in Table 1, the thermal stability of the N_{TB} phase exhibits some dependence on the chemical makeup of both the central spacer and the linking units. Previously, we reported that the incidence of the N_{TB} phase has its origins in the bend-angle of the dimer. We opted previously to use the all-*trans* conformer to obtain the crucial inter-aromatic angle of the dimers, and while this appears to be the dominant conformer by solution based 1D ¹H NOESY NMR, this obviously fails to capture any information concerning the distribution of conformers. Given the large number of possible conformers (N^m ; where *N* is the number of torsions allowed to rotate and *m* is the number of rotations about each dihedral; so for CB11CB – which has 10 dihedrals in its spacer – assuming threefold rotation gives $3^{10} = 59,049$ conformers, some of which will be degenerate), we considered the use of semi-empirical computational methods to explore the conformational landscape. We chose to study butane as a model compound for two reasons: first, as it is composed of a small number of atoms (C₄H₁₀), calculations are computationally inexpensive, and second, this torsion has been studied extensively by both theory and experiment. We studied the C–C–C–C torsion by performing fully relaxed scans (72° × 5°) at various levels of theory. Plots of energy (kJ mol^{−1}) versus the dihedral angle using various computational methods are given in Figure 2.

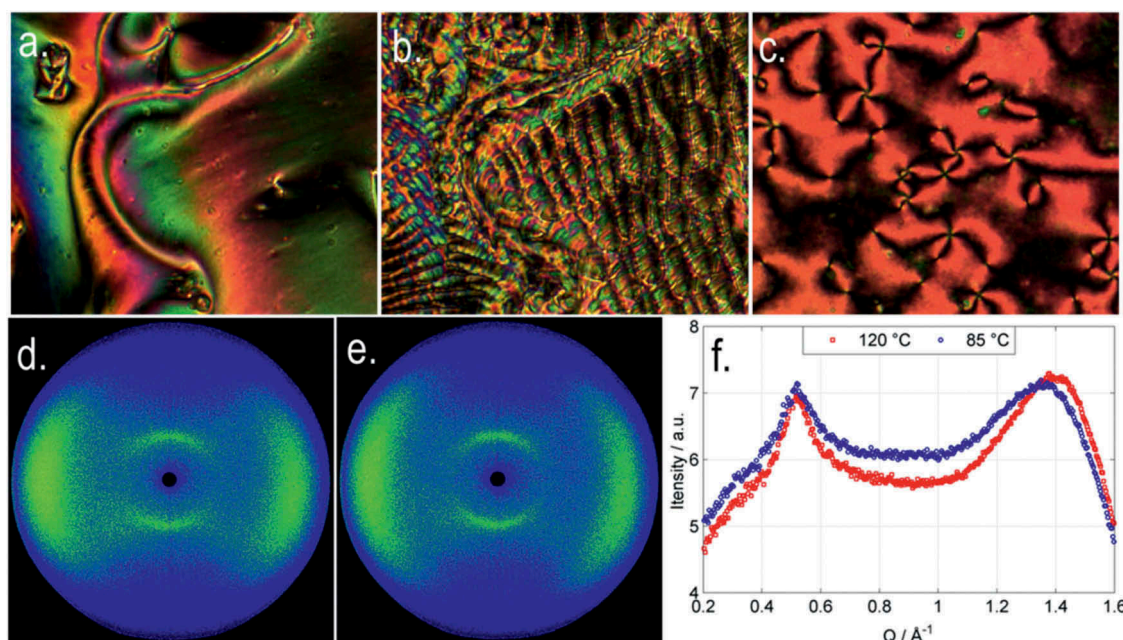


Figure 1. (Colour online) Photomicrographs (×100, crossed polars) of (a) the nematic phase of **5** at 130°C, (b) the twist-bend phase of **5** at 91°C, (c) the nematic phase of **10** at 100°C, (d) two-dimensional SAXS pattern obtained for a magnetically aligned sample of **5** in the nematic phase at 120°C, (e) two-dimensional SAXS pattern obtained for the twist-bend phase of **5** at 85°C, (f) plot intensity versus scattering vector Q for the N and twist-bend phase of **5** obtained by radially averaging of the two-dimensional SAXS patterns (0.05° step size).

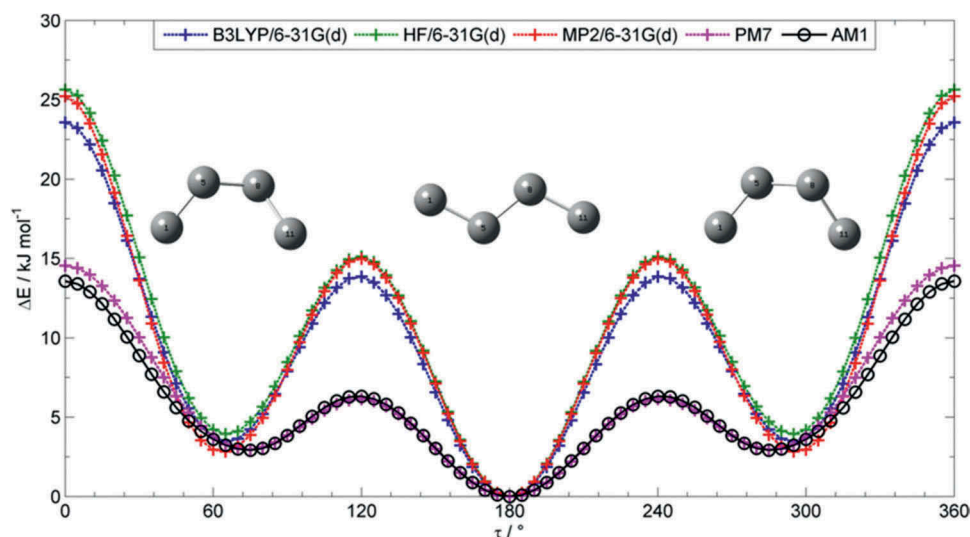


Figure 2. (Colour online) Plot of energy (kJ mol^{-1}) as a function of the C–C–C torsion of butane ($72 \times 5^\circ$ steps) as obtained at various levels of theory (DFT(B3LYP/6-31G(d)), HF/6-31G(d), MP2/6-31G(d), PM7, AM1). Optimised geometries for *gauche* and *trans* conformers as obtained at the MP2/6-31G(d) level are overlaid.

As shown in Table 2, the semi-empirical methods (PM7 and AM1) provide lower values for the heights of both the eclipse barrier (E_{0°) and the *trans*–*gauche* barrier (E_{120°) than the other computational methods used. As we will assume threefold rotation about each bond when studying bimesogens, the most relevant value is the energy difference between the *trans* and

gauche forms, and experimental data for these are available from electron diffraction and solid phase IR. Hartree–Fock and DFT(B3LYP) calculations (6-31G(d) basis set) appear to overestimate the *trans*–*gauche* energy difference, while MP2/6-31G(d) gives a value that is slightly lower. Calculations at the computationally expensive MP4(SDTQ)/6-31G*/MP2/6-31G(d)

Table 2. Comparison of rotational barrier energies for butane (in kJ mol^{-1}) using various methods, along with experimentally obtained values.

Method	ΔE_{t-g}	E_{120°	E_{0°	CPU time	Ref.
IR in solid Ne	3.087	–	–	–	[46]
Electron diffraction	3.184	–	–	–	[47]
AM1	2.961	6.317	13.57	00:01:53	This work
PM7	2.922	6.146	14.54	00:01:47	This work
HF/6-31G(d)	3.938	15.120	25.64	00:15:30	This work
B3LYP/6-31G(d)	3.469	13.850	23.58	01:36:36	This work
MP2/6-31G(d)	2.839	14.990	25.21	03:20:06	This work
CCSD(T)/TZ(2d,2p)	2.509	13.701	23.253	–	[48]
RMP2/QD(2d1f,2p1d)	2.798	13.701	23.832	–	[48]
MP4(SDTQ)/6-31G*//MP2/6-31G(d)	2.991	14.859	24.797	–	[48]
QCISD(T).6-31G*//MP2/6-31G(d)	2.991	14.666	24.604	–	[48]

The 'time' refers to the total CPU time used for in calculations for data obtained in this work and is given in HH:MM:SS.

and QCISD(T).6-31G*//MP2/6-31G(d) levels gives values that are close to those obtained by experiment. Remarkably, the energy *trans*–*gauche* difference calculated at the AM1 and PM7 semi-empirical methods is only marginally smaller than that of the experiment and the more computationally expensive MP4/QCISD methods. Thus, as both semi-empirical methods give reasonable values for ΔE_{t-g} , they can be used for a computationally inexpensive study of the conformational landscape of liquid-crystalline dimers, with the caveat that we are assuming a threefold rotation of each dihedral in the spacer unit ($\tau = 90, 180, 270$). We opted to use the AM1 method as implemented in Gaussian G09.e01 as it is marginally closer to experimental values than PM7 (as implemented in MOPAC 2012).

Using the semi-empirical AM1 method (as implemented in Gaussian G09.e01), we performed relaxed scans about each of the rotatable bonds in the spacers of compounds **3**–**10**, giving a library of conformers for each (as **1** and **2** are non-mesogenic, we excluded these compounds from our study). Output files were read by a Matlab script which extracted the Cartesian coordinates and the energy of the final optimised geometry. Conformers were discarded if their energy was greater than that of the lowest energy conformer by 20 kJ mol^{-1} or more. From the Cartesian coordinates, the angle between the two mesogenic units was calculated. Using a Boltzman distribution (300 K; for a conformer whose energy is 20 kJ mol^{-1} higher than that of the ground state conformer, there is a Boltzmann population ratio of ~ 0.0003 for the two states), we obtain a probability for each given angle as show in the histogram plot in Figure 3. By weighting each angle with its probability we obtain an 'average curvature' for each molecule; while we observe for each material – with the exception of **10** – that the all *trans*

form is the energy minimum the use of a weighted bend-angle is much more realistic than our previous use of a single all *trans* conformer [36]. It is only right to point out that this method is not without limitations; first, DFT or MP2 calculations are probably preferable over semi-empirical methods, second, these calculations are performed on isolated molecules rather than in a condensed phase, and lastly, the use of discrete conformers (as employed here) is less realistic than using continuous torsional potentials. The conformer distributions presented by us – the difference between semi-empirical and DFT/MP2 geometries notwithstanding – appear to be on trend with those reported for CB7CB and CB6OCB [24].

Although there are differences in the conformer distributions of each material, all broadly follow the same trend, with the majority of conformers having a bend angle between 90° and 135° : For compound **3**, 80% of conformers lie within this range; 60% for **4**; 81% for **5**; 79% for **6**; 85% for **8**. There is a significant probability associated with hairpin conformers (defined arbitrarily here as a bend angle of below 45°) in compounds **3**–**6**, being as high as 28% for **4**; however, for compound **9**, the probability of a conformer with a bend angle below 45° is significantly smaller ($<1\%$). For all materials are also low probabilities of 'linear conformers' (defined here as a bend angle of $>150^\circ$) that can result from having two or more *gauche* conformations in the spacer. As discussed above, using a Boltzman-weighted inter-aromatic angle for compounds **3**–**10** gives a more realistic value of this bend angle than the single conformer (all *trans*) used by us previously. A plot of $T_{N_{TB-N}}$ and $T_{N_{Iso}}$ versus this average inter-aromatic angle is given in Figure 4. Again, the thermal stability of the N_{TB} phase (judged by its onset temperature) would appear to exhibit a dependence on the bend angle of the dimer.

For compounds **3**–**9**, the minimum energy conformer (determined using the AM1 semi-empirical method) is the all *trans* form; however for **10**, the diethyleneoxy spacer of the lowest energy conformer has four torsions in the *gauche* conformation. This behaviour of **10** mirrors the behaviour of low molecular weight dimethyl ethylene oxides [49]. Although the average bend angle of **10** is calculated to be comparable to that of **3** ($3 = 103^\circ$, $10 = 105^\circ$), the values of $T_{N-N_{TB}}$ are vastly different. Due to the preference for *gauche* conformers, the distribution of bend angles for compound **10** is extremely broad, whereas for **3** (and indeed compounds **4**–**9**, see Figure 5), the majority of bend-angles lie in the range 90 – 120° . The difference in $T_{N-N_{TB}}$ can therefore be attributed to the difference in conformational landscape, and while the average bend would appear to be important to determining, $T_{N-N_{TB}}$

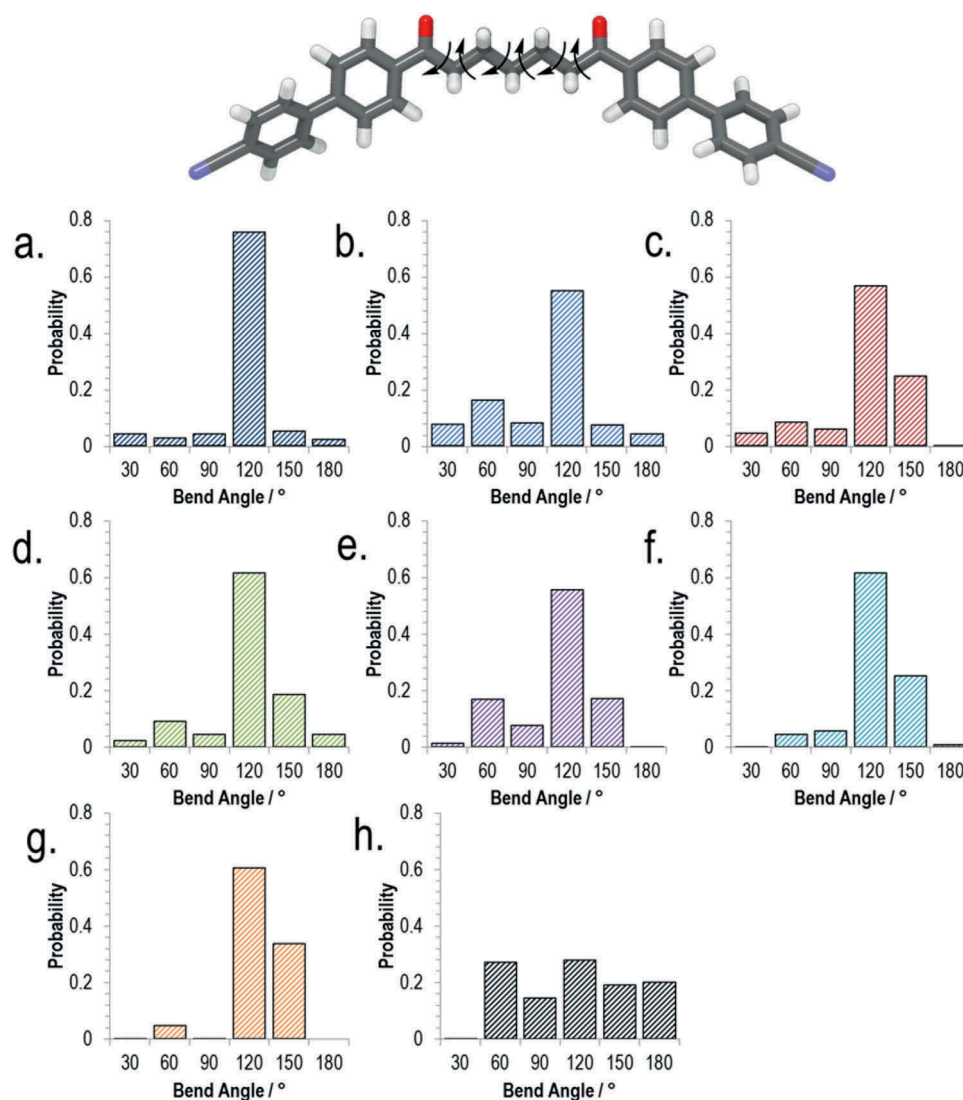


Figure 3. (Colour online) Top, the AM1 minimised all-trans form of compound **8** with arrows showing the bonds allowed to undergo threefold rotation during the conformer search (total of 729 conformers). Bottom, histogram plots (bin size 30°) of the probability of a given intermesogen angle as determined using the AM1 semi-empirical method for compounds: **3** (a), **4** (b), **5** (c), **6** (d), **7** (e), **8** (f), **9** (g), **10** (h).

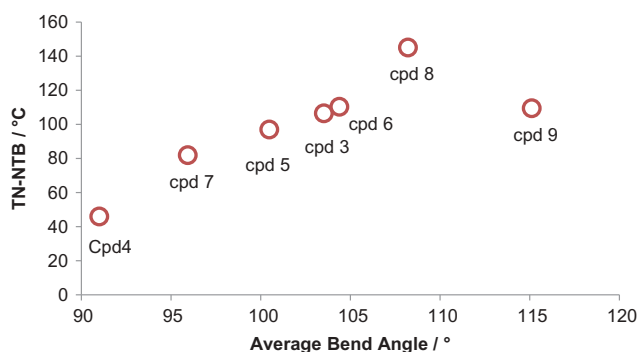


Figure 4. (Colour online) Plot of T_{N-NTB} (for cpd **9** $T_{N_{TB-ISO}}$ is plotted instead, see text) transition temperatures versus the Boltzman-weighted interatomic angle for compounds **3**–**9**, determined on isolated molecules using the AM1 semi-empirical method as described in the text.

this only applies where the distribution of conformers is centred on this particular value – for **10**, the average bend is heavily skewed by the presence of both bent and linear conformers. This is an important design feature to be considered when preparing new twist-bend materials; control of molecular structure affords control over the conformational landscape (and the average molecular bend) and these appear to dictate the incidence of this phase.

Conclusions

We have synthesised several novel dimeric materials with varying linking-group and spacer composition with the aim of exploring how molecular structure,

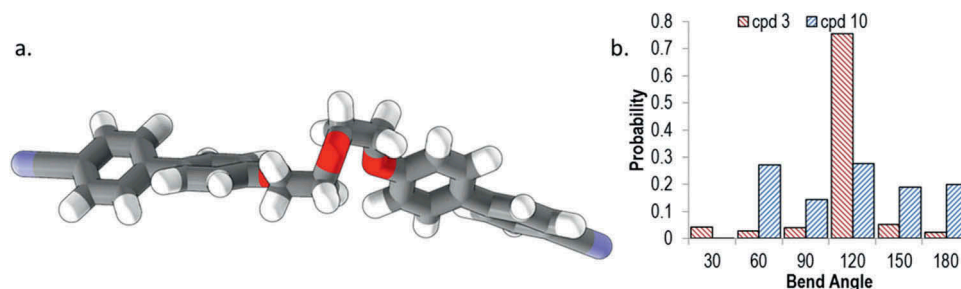


Figure 5. (Colour online) (a) Minimum energy conformer of **10** obtained using the AM1 semi-empirical method (bend angle of 117°) and (b) histogram plot of the probability of a given intermesogen angle as determined using the AM1 semi-empirical method for compounds **3** and **10** as described in the text.

specifically the bend-angle of the dimer, impacts upon the incidence of the currently topical twist-bend phase. In doing so, we have discovered another example of a material exhibiting a direct isotropic-to-twist-bend phase transition, however, the monotropic nature of this phase transition renders this material somewhat difficult to study. The mesogenic compounds **3–10** were studied computationally; we performed relaxed scans about each of the rotatable bonds in the spacers, giving a library of conformers for each compound from which we could obtain a Boltzmann-weighted bend-angle for each material. This improves on our earlier demonstration of a link between the degree of bend and the thermal stability of the N_{TB} phase by capturing information about the conformational landscape, with the present results serving to confirm that the twist-bend phase does indeed exhibit a dependency on the bend-angle. However, this is not the only factor that must be considered; compounds **3** (CB7CB) and **10** (CBO2O2OCB) have similar bend-angles (103° and 105°, respectively), but **3** exhibits a somewhat narrow distribution of conformers centred around 90–120°, we find that **10** exhibits an almost uniform distribution across all angles. The result is that compound **3** exhibits the twist-bend phase, but compound **10** does not. Thus, we feel it is likely that it is the gross shape of the molecule (and possibly the free volume [50]) that dictates the incidence of the twist-bend phase. It is presently an open question as to how changes in the average bend angle impact on the properties and structure of the twist bend phase, e.g. pitch length, conical angle, viscosity; however, it would be surprising if these were not dependent to some extent.

Acknowledgements

CTA thanks the University of York for the award of a doctoral scholarship. The EPSRC is thanked for funding the

Bruker D8 small-angle X-ray scattering instrument used in this work via grant EP/K039660/1.

Disclosure statement

No potential conflict of interest was reported by the authors.

Funding

This work was supported by the Engineering and Physical Sciences Research Council: [grant EP/K039660/1].

ORCID

Richard J. Mandle  <http://orcid.org/0000-0001-9816-9661>

References

- [1] Paterson DA, Xiang J, Singh G, et al. Reversible isothermal twist-bend nematic-nematic phase transition driven by the photoisomerization of an azobenzene-based non-symmetric liquid crystal dimer. *J Am Chem Soc.* 2016;138(16):5283–5289.
- [2] Zhang ZP, Panov VP, Nagaraj M, et al. Raman scattering studies of order parameters in liquid crystalline dimers exhibiting the nematic and twist-bend nematic phases. *J Mater Chem C.* 2015;3(38):10007–10016.
- [3] Sebastian N, Lopez DO, Robles-Hernandez B, et al. Dielectric, calorimetric and mesophase properties of 1''-(2',4'-difluorobiphenyl-4'-yloxy)-9''-(4'-cyanobiphenyl-4'-yloxy) nonane: an odd liquid crystal dimer with a monotropic mesophase having the characteristics of a twist-bend nematic phase. *Phys Chem Chem Phys.* 2014;16(39):21391–21406.
- [4] Chen D, Nakata M, Shao R, et al. Twist-bend heliconical chiral nematic liquid crystal phase of an achiral rigid bent-core mesogen. *Phys Rev E Stat Nonlin Soft Matter Phys.* 2014;89(2):022506.
- [5] Zep A, Aya S, Aihara K, et al. Multiple nematic phases observed in chiral mesogenic dimers. *J Mater Chem C.* 2013;1(1):46–49.

- [6] Chen D, Porada JH, Hooper JB, et al. Chiral heliconical ground state of nanoscale pitch in a nematic liquid crystal of achiral molecular dimers. *Proc Natl Acad Sci U S A*. 2013;110(40):15931–15936.
- [7] Borshch V, Kim YK, Xiang J, et al. Nematic twist-bend phase with nanoscale modulation of molecular orientation. *Nat Commun*. 2013;4:2635.
- [8] Adlem K, Copic M, Luckhurst GR, et al. Chemically induced twist-bend nematic liquid crystals, liquid crystal dimers, and negative elastic constants. *Phys Rev E*. 2013;88(2).
- [9] Henderson PA, Imrie CT. Methylene-linked liquid crystal dimers and the twist-bend nematic phase. *Liq Cryst*. 2011;38(11–12):1407–1414.
- [10] Cestari M, Diez-Berart S, Dunmur DA, et al. Phase behavior and properties of the liquid-crystal dimer 1'',7''-bis(4-cyanobiphenyl-4'-yl) heptane: a twist-bend nematic liquid crystal. *Phys Rev E Stat Nonlin Soft Matter Phys*. 2011;84(3 Pt 1):031704.
- [11] Šepelj M, Lesac A, Baumeister U, et al. Intercalated liquid-crystalline phases formed by symmetric dimers with an alpha,omega-diiminoalkylene spacer. *J Mater Chem*. 2007;17(12):1154–1165.
- [12] Šepelj M, Lesac A, Baumeister U, et al. Dimeric salicylaldehyde-based mesogens with flexible spacers: parity-dependent mesomorphism. *Chem Mater*. 2006;18(8):2050–2058.
- [13] Dozov I. On the spontaneous symmetry breaking in the mesophases of achiral banana-shaped molecules. *Europhys Lett*. 2001;56(2):247–253.
- [14] Zhu C, Tuchband MR, Young A, et al. Resonant Carbon K-edge soft X-ray scattering from lattice-free heliconical molecular ordering: soft dilative elasticity of the twist-bend liquid crystal phase. *Phys Rev Lett*. 2016;116(14):147803.
- [15] Mandle RJ, Davis EJ, Archbold CT, et al. Microscopy studies of the nematic NTB phase of 1,11-di-(1''-cyanobiphenyl-4-yl)undecane. *J Mater Chem C*. 2014;2(3):556–566.
- [16] Archbold CT, Davis EJ, Mandle RJ, et al. Chiral dopants and the twist-bend nematic phase—induction of novel mesomorphic behaviour in an apolar bimesogen. *Soft Matter*. 2015;11(38):7547–7557.
- [17] Mandle RJ, Cowling SJ, Goodby JW. A nematic to nematic transformation exhibited by a rod-like liquid crystal. *Phys Chem Chem Phys*. 2017;19(18):11429–11435.
- [18] Mandle RJ. The shape of things to come: the formation of modulated nematic mesophases at various length scales. *Chem Eur J*. 2017;23:8771–8779.
- [19] Mandle RJ. The dependency of twist-bend nematic liquid crystals on molecular structure: a progression from dimers to trimers, oligomers and polymers. *Soft Matter*. 2016;12(38):7883–7901.
- [20] Panov VP, Vij JK, Mehl GH. Twist-bend nematic phase in cyanobiphenyls and difluoroterphenyls bimesogens. *Liq Cryst*. 2017;44(1):147–159.
- [21] Ivšić T, Baumeister U, Dokli I, et al. Sensitivity of the NTB phase formation to the molecular structure of imino-linked dimers. *Liq Cryst*. 2017;44(1):93–105.
- [22] Archbold CT, Andrews JL, Mandle RJ, et al. Effect of the linking unit on the twist-bend nematic phase in liquid crystal dimers: a comparative study of two homologous series of methylene- and ether-linked dimers. *Liq Cryst*. 2017;44(1):84–92.
- [23] Abberley JP, Jansze SM, Walker R, et al. Structure-property relationships in twist-bend nematogens: the influence of terminal groups. *Liq Cryst*. 2017;44(1):68–83.
- [24] Paterson DA, Gao M, Kim Y-K, et al. Understanding the twist-bend nematic phase: the characterisation of 1-(4-cyanobiphenyl-4'-yl)oxy-6-(4-cyanobiphenyl-4'-yl)hexane (CB6OCB) and comparison with CB7CB. *Soft Matter*. 2016;12(32):6827–6840.
- [25] Mandle RJ, Voll CCA, Lewis DJ, et al. Etheric bimesogens and the twist-bend nematic phase. *Liq Cryst*. 2016;43(1):13–21.
- [26] Mandle RJ, Goodby JW. Dependence of mesomorphic behaviour of methylene-linked dimers and the stability of the N-TB/N-X phase upon choice of mesogenic units and terminal chain length. *Chem-Eur J*. 2016;22(27):9366–9374.
- [27] Mandle RJ, Goodby JW. A twist-bend nematic to an intercalated, anticlinic, biaxial phase transition in liquid crystal bimesogens. *Soft Matter*. 2016;12(5):1436–1443.
- [28] Mandle RJ, Davis EJ, Voll CCA, et al. The relationship between molecular structure and the incidence of the N-TB phase. *Liq Cryst*. 2015;42(5–6):688–703.
- [29] Mandle RJ, Davis EJ, Archbold CT, et al. Apolar bimesogens and the incidence of the twist-bend nematic phase. *Chem Eur J*. 2015;21(22):8158–8167.
- [30] Mandle RJ, Davis EJ, Lobato SA, et al. Synthesis and characterisation of an unsymmetrical, ether-linked, fluorinated bimesogen exhibiting a new polymorphism containing the NTB or 'twist-bend' phase. *Phys Chem Chem Phys*. 2014;16(15):6907–6915.
- [31] Mandle RJ, Goodby JW. A liquid crystalline oligomer exhibiting nematic and twist-bend nematic mesophases. *Chemphyschem*. 2016;17(7):967–970.
- [32] Wang Y, Singh G, Agra-Kooijman DM, et al. Room temperature heliconical twist-bend nematic liquid crystal. *Crystengcomm*. 2015;17(14):2778–2782.
- [33] Jansze SM, Martinez-Felipe A, Storey JM, et al. A twist-bend nematic phase driven by hydrogen bonding. *Angew Chem Int Ed Engl*. 2015;54(2):643–646.
- [34] Mandle RJ, Goodby JW. Progression from nano to macro science in soft matter systems: dimers to trimers and oligomers in twist-bend liquid crystals. *Rsc Adv*. 2016;6(41):34885–34893.
- [35] Mandle RJ, Goodby JW. Does topology dictate the incidence of the twist-bend phase? Insights gained from novel unsymmetrical bimesogens. *Chem-Eur J*. 2016;22(51):18456–18464.
- [36] Mandle RJ, Archbold CT, Sarju JP, et al. The dependency of nematic and twist-bend mesophase formation on bend angle. *Sci Rep-UK*. 2016;6:36682.
- [37] Frisch MJ, Trucks GW, Schlegel HB, et al. Gaussian 09. Wallingford (CT): Gaussian; 2009.
- [38] Tarini M, Cignoni P, Montani C. Ambient occlusion and edge cueing to enhance real time molecular visualization. *IEEE T Vis Comput Gr*. 2006;12(5):1237–1244.

- [39] Mandle RJ, Davis EJ, Voll CCA, et al. Self-organisation through size-exclusion in soft materials. *J Mater Chem C*. 2015;3(10):2380–2388.
- [40] Emsley JW, Luckhurst GR, Shilstone GN, et al. The preparation and properties of the Alpha,Omega-Bis(4,4'-Cyanobiphenyloxy)alkanes - nematogenic molecules with a flexible core. *Mol Cryst Liq Cryst*. 1984;102(8–9):223–233.
- [41] Creed D, Gross JRD, Sullivan SL, et al. Effect of molecular-structure on mesomorphism .18. Twin dimers having methylene, ethylene-oxide and siloxane spacers. *Mol Cryst Liq Cryst*. 1987;149:185–193.
- [42] Paterson DA, Abberley JP, Harrison WT, et al. Cyanobiphenyl-based liquid crystal dimers and the twist-bend nematic phase. *Liq Cryst*. 2017;44(1):127–146.
- [43] Ramou E, Ahmed Z, Welch C, et al. The stabilisation of the N_x phase in mixtures. *Soft Matter*. 2016;12(3):888–899.
- [44] Dawood AA, Grossel MC, Luckhurst GR, et al. On the twist-bend nematic phase formed directly from the isotropic phase. *Liq Cryst*. 2016;43(1):2–12.
- [45] Dawood AA, Grossel MC, Luckhurst GR, et al. Twist-bend nematics, liquid crystal dimers, structure-property relations. *Liq Cryst*. 2017;44(1):106–126.
- [46] Kanesaka I, Snyder RG, Strauss HL. Experimental-determination of the trans-gauche energy difference of gaseous N-pentane and diethyl-ether. *J Chem Phys*. 1986;84(1):395–397.
- [47] Heenan RK, Bartell LS. Electron-diffraction studies of supersonic jets .4. Conformational cooling of normal-butane. *J Chem Phys*. 1983;78(3):1270–1274.
- [48] Tsuzuki S, Uchimar T, Tanabe K. Conformational-analysis of N-alkanes using density-functional theory - comparison with Ab-initio calculations. *Chem Phys Lett*. 1995;246(1–2):9–12.
- [49] Sasanuma Y, Sugita K. The attractive gauche effect of ethylene oxides. *Polym J*. 2006;38(9):983–988.
- [50] Goodby JW, Mandle RJ, Davis EJ, et al. What makes a liquid crystal? The effect of free volume on soft matter. *Liq Cryst*. 2015;42(5–6):593–622.